6

ESTIMATION OF PERMITTIVITIES OF SOLIDS FROM MEASUREMENTS ON PULVERIZED OR GRANULAR MATERIALS

S. O. Nelson

6.1 Introduction
6.2 Dielectric Mixture Equations
6.3 Density Dependence of Particulate Material Permittivity
6.4 Experimental Data
a. Measurement Methods
b. Processing of Data for Extrapolation to Solid Density
6.5 Examples of Applications
6.6 Comparison of Extrapolation and Mixture-Equation Predictions
a. General Comparisons
b. Particle Size and Shape Variation
c. Comparison of Predicted with Known Permittivities
6.7 Conclusions
Acknowledgements
References

6.1 Introduction

Often it is difficult to determine the permittivities of solid materials because of difficulty in machining samples of some materials to the precise dimensions required for the measurement, because they do not exist in solid form of sufficient size for the required measurement, or because, in the case of some minerals, they cannot be obtained in pure form without pulverization and purification. For these reasons, efforts have been devoted to the study of several dielectric mixture equations for the correlation of the permittivity of solid materials with those

obtained from measurements on powdered or pulverized materials [1–5].

A simple method has been developed for extrapolation of permittivity measurements data on pulverized materials at known bulk densities to obtain the permittivities of the solid material at its known density [6–7]. The basis for this method will be described, and comparisons will be made with the permittivity values predicted by several of the well-known dielectric mixture equations for several different materials.

In this chapter we will be dealing entirely with the complex permittivity relative to free space, $\epsilon = \epsilon' - j\epsilon''$. The real part is referred to as the dielectric constant, and the imaginary part is the dielectric loss factor. The absolute complex permittivity, if desired, is obtained by multiplying the relative complex permittivity by the permittivity of free space, $\epsilon_0 = 8.854 \times 10^{-12}$farad/m. The loss tangent of the dielectric material is $\tan\delta = \epsilon''/\epsilon'$, where δ is the dielectric loss angle of the material, and conductivity in siemens/m is $\sigma = \omega\epsilon_0\epsilon''$, where $\omega = 2\pi f$ is the angular frequency of the applied alternating electric field of frequency f in hertz.

6.2 Dielectric Mixture Equations

First, the equations for heterogeneous mixtures that are considered in this work will be identified. For an understanding of their origins and bases, the reader is referred to a number of notable reviews and summaries relating to this topic [8–16]. The notation used here applies to two-component mixtures where ϵ represents the complex permittivity of the mixture, ϵ_1 is the permittivity of the medium in which particles of permittivity ϵ_2 are dispersed, and v_1 and v_2 are the volume fractions of the respective components, where $v_1 + v_2 = 1$.

The earliest equation of the group considered here is often termed the complex refractive index mixture equation, since it was originally applied in optics [17–19]. The same equation has been arrived at by a number of researchers [5], [20–21] considering plane wave propagation through a heterogeneous dielectric mixture. This equation has been relatively successful in many applications [20–27]. The equation implies the additivity of the square roots of the permittivities of the constituents of a mixture when taken in proportion to their volume fractions.

$$\sqrt{\epsilon} = v_1\sqrt{\epsilon_1} + v_2\sqrt{\epsilon_2} \tag{1}$$

An equation developed by Landau and Lifshitz [28] and Looyenga [29], independently and from different approaches, implies the additivity of the cube roots of the permittivities of the mixture constituents when taken in proportion to their volume fractions.

$$(\epsilon)^{1/3} = v_1(\epsilon_1)^{1/3} + v_2(\epsilon_2)^{1/3} \tag{2}$$

This equation too has been used with good success on some powdered materials [3], [14], [15], [30], [31].

A widely used mixture equation is that of Böttcher [1, 15], which has been studied and recommended for use with powdered materials [2, 4, 31].

$$\frac{\epsilon - \epsilon_1}{3\epsilon} = v_2 \frac{\epsilon_2 - \epsilon_1}{\epsilon_2 + 2\epsilon} \tag{3}$$

Another very well known mixture equation is that originally reported by Bruggeman [32] and extended to complex permittivities by Hanai [33].

$$\frac{\epsilon - \epsilon_2}{\epsilon_1 - \epsilon_2} \left(\frac{\epsilon_1}{\epsilon}\right)^{1/3} = 1 - v_2 \tag{4}$$

Another very early mixture equation was the Rayleigh [34] equation.

$$\frac{\epsilon - \epsilon_1}{\epsilon + 2\epsilon_1} = v_2 \frac{\epsilon_2 - \epsilon_1}{2\epsilon_1 + \epsilon_2} \tag{5}$$

The Lichtenecker [19, 35] logarithmic mixture equation was another often applied to mixtures with particles of arbitrary shape.

$$\ln \epsilon = v_1 \ln \epsilon_1 + v_2 \ln \epsilon_2 \tag{6}$$

These are the six dielectric mixture equations considered in predicting the permittivities of solid materials from measurements of permittivity of particulate materials in this chapter. The corresponding forms of these equations for calculating the complex permittivities of the solid material from measurements on the air-particle mixtures ($\epsilon_1 = 1 - j0$ for air) are as follows:

Refractive Index, (1)

$$\epsilon_2 = \left(\frac{\sqrt{\epsilon} + v_2 - 1}{v_2}\right)^2 \tag{7}$$

Landau & Lifshitz, Looyenga, (2)

$$\epsilon_2 = \left(\frac{\epsilon^{1/3} + v_2 - 1}{v_2} \right)^3 \tag{8}$$

Böttcher, (3)

$$\epsilon_2 = \frac{\epsilon[3v_2 + 2(\epsilon - 1)]}{3v_2\epsilon - (\epsilon - 1)} \tag{9}$$

Bruggeman-Hanai, (4)

$$\epsilon_2 = \frac{1 - v_2 - \epsilon^{2/3}}{1 - v_2 - \epsilon^{-1/3}} \tag{10}$$

Rayleigh, (5)

$$\epsilon_2 = \frac{v_2(\epsilon + 2) + 2(\epsilon - 1)}{v_2(\epsilon + 2) - (\epsilon - 1)} \tag{11}$$

Lichtenecker, (6)

$$\epsilon_2 = e^{\left(\frac{\ln \epsilon}{v_2}\right)} \tag{12}$$

where e is the base of the natural logarithms.

6.3 Density Dependence of Particulate Material Permittivity

Essentially linear functions of the real and imaginary components of the complex permittivity of particulate materials such as pulverized coal, wheat, and whole-wheat flour were identified previously [30]. These findings were based on earlier work in which Klein [36] observed the linearity of $\sqrt{\epsilon'}$ with the bulk density of granular coal, and in which Kent [37], working with fish meal, found that ϵ' and ϵ'' were both quadratic functions of the bulk density of the fish meal as follows:*

$$\epsilon' = a\rho^2 + b\rho + 1 \tag{13}$$

$$\epsilon'' = c\rho^2 + d\rho \tag{14}$$

* (13) and (14) are equivalent to expressing the relative complex permittivity as a quadratic function of bulk density, $\epsilon = a^*\rho^2 + b^*\rho + 1$, where the constants $a^* = a - jc$ and $b^* = b - jd$ are complex numbers.

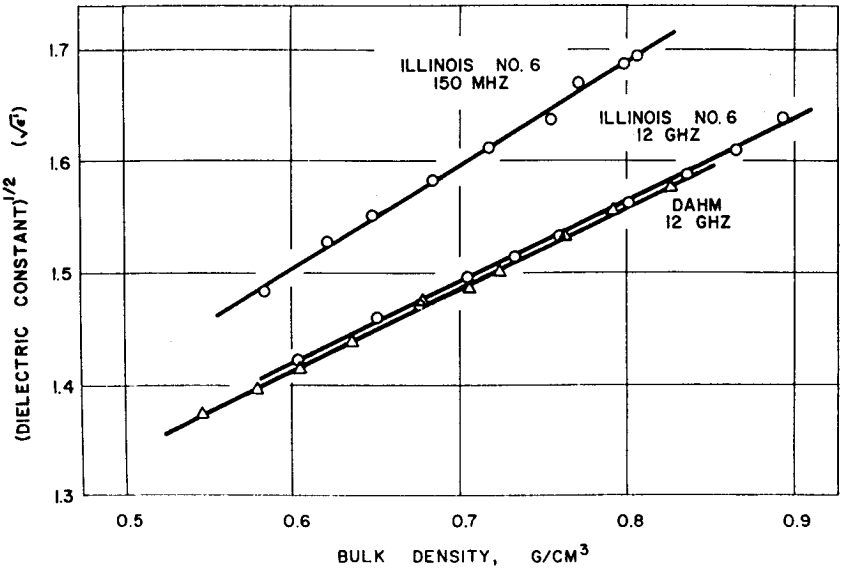

Figure 6.1 Linear relationships between the square root of the dielectric constant and bulk density for indicated dry, pulverized run-of-mine coal samples at indicated frequencies at 22° C [38].

where ρ represents the density of the air-particle mixture, a, b, c, and d are constants for a given particulate material and ϵ' and ϵ'' have values of 1 and 0, respectively, for air alone ($\rho = 0$). The linearity of ϵ' with bulk density was confirmed with data on pulverized coal [38], and these data are shown in Fig. 6.1. These relationships are expressed as

$$\sqrt{\epsilon'} = m\rho + 1 \tag{15}$$

Equations (13) and (15) are equivalent if $a = m^2$ and $b = 2m$. Thus, if these relationships are true, measurement of the dielectric constant of a particulate material at a given density, along with the ($\rho = 0$, $\epsilon' = 1$) intercept, provides information on the dielectric constant at all densities, including that of the solid material if its density is known. Examining the expression for the loss factor, (14), the square can be completed by adding a constant e to each side, and a linear function of ϵ'' is obtained

$$\sqrt{\epsilon'' + e} = \sqrt{c}\rho + \sqrt{e} \tag{16}$$

$$e = d^2/4c \tag{17}$$

Thus, to describe the density dependence of the complex permittivity of a particulate material, one needs to obtain the values for a, b, c,

Material	Freq., GHz	Measured properties				Vol. frac.
		Density, g/cm^3		Permittivity, Particulate		
		Solid	Partic.			
		ρ_2	ρ	ϵ'	ϵ''	v_2
Whole-kernel	9.4	1.437	.730	2.45	.22	.51
hard red			.778	2.59	.25	.54
winter wheat			.887	2.95	.33	.62
11.5% m.c.			.955	3.18	.37	.66
cv. 'Scout 66'			1.067	3.54	.46	.74
[30]			1.178	3.97	.57	.82
			1.271	4.34	.69	.88
Ground	11.7	1.406	.592	2.07	.14	.42
hard red			.694	2.31	.19	.49
winter wheat			.743	2.44	.22	.53
10.9% m.c.			.797	2.61	.24	.57
cv. 'Scoutland'			.883	2.88	.30	.63
[30]			.938	3.05	.36	.67
			.994	3.18	.40	.71
			1.060	3.36	.42	.75
			1.105	3.53	.43	.79
			1.148	3.70	.47	.82
Ground	11.0	1.476	.696	2.38	.26	.47
white rice			.748	2.53	.30	.51
12.2% m.c.			.811	2.70	.34	.55
cv. 'Lebonnet'			.905	2.97	.44	.61
[46]			1.011	3.27	.51	.68
			1.135	3.62	.59	.77
			1.228	4.02	.68	.83

Table 6.1a Comparison of permittivities of cereal grain kernels estimated by extrapolation of linear density functions of the dielectric constant and loss factor with those predicted by indicated mixture equations from permittivity measurements on bulk samples of whole-kernel grain and ground grain at 24° C. Tabular data rounded to one, two, three, or four decimal places. All calculations performed on unrounded data.

and d. Measurement of the permittivity of the particulate material at a given density establishes slope m of (15), thus determining values for a and b. Measurements at a few additional densities are necessary for determination of c and d, as will be explained later.

It is interesting to note that (13) and (15) are consistent with the refractive index mixture equation (1), when used for the real part of

Estimated complex permittivity of solid material						
Extrapolation of linear functions†			Mixture equations			
$(\epsilon')^{1/2}$	$(\epsilon')^{1/3}$	$(\epsilon''+\epsilon)^{1/2}$	RI		LLL	
ϵ'	ϵ'	ϵ''	ϵ'	ϵ''	ϵ'	ϵ''
4.81±.27	4.98±.13	.85±.04	4.46	.59	4.77	.68
			4.52	.61	4.82	.69
			4.67	.68	4.93	.76
			4.73	.69	4.96	.76
			4.78	.71	4.96	.77
			4.88	.77	5.01	.82
			4.95	.83	5.03	.86
4.49±.14	4.64±.09	.71±.06	4.17	.49	4.51	.57
			4.18	.51	4.49	.59
			4.25	.54	4.53	.62
			4.35	.55	4.61	.63
			4.44	.59	4.67	.66
			4.48	.66	4.69	.73
			4.44	.67	4.62	.71
			4.43	.64	4.57	.69
			4.49	.62	4.61	.66
			4.54	.63	4.65	.67
4.78±.14	4.97±.12	.94±.07	4.63	.75	5.00	.89
			4.67	.79	5.02	.92
			4.71	.83	5.03	.95
			4.75	.90	5.02	1.01
			4.74	.90	4.96	.99
			4.72	.88	4.87	.94
			4.87	.90	4.98	.94

Table 6.1b Continuation of Table 6.1. "RI" = "Refractive Index." "LLL" = "Landau & Lifshitz, Looyenga." †Calculated values with extrapolated 95% confidence intervals.

the complex permittivity. Since $v_2 = \rho/\rho_2$, where ρ is the density of the air-particle mixture, and ρ_2 is the density of the particles, this substitution in (1) yields the following for an air-particle mixture:

$$\sqrt{\epsilon'} = \frac{\sqrt{\epsilon_2'} - 1}{\rho_2}\rho + 1 \tag{18}$$

which is equivalent to (15), where $m = (\sqrt{\epsilon_2'} - 1)/\rho_2$. In an analogous manner, it can be shown that the linearity of the cube root of the di-

Material	Estimated complex permittivity of solid material			
	Mixture equations			
	B		BH	
	ϵ'	ϵ''	ϵ'	ϵ''
Whole–kernel	4.74	.67	5.26	.91
hard red	4.76	.67	5.27	.90
winter wheat	4.82	.71	5.29	.93
11.5% m.c.	4.84	.71	5.26	.90
cv. 'Scout 66'	4.84	.72	5.17	.86
[30]	4.90	.77	5.14	.88
	4.95	.82	5.11	.90
Ground	4.56	.59	5.05	.82
hard red	4.47	.58	4.91	.78
winter wheat	4.48	.60	4.91	.80
10.9% m.c.	4.54	.60	4.97	.89
cv. 'Scoutland'	4.58	.62	4.96	.79
[30]	4.58	.68	4.93	.85
	4.52	.68	4.81	.82
	4.48	.65	4.72	.76
	4.52	.62	4.75	.72
	4.56	.63	4.76	.72
Ground	4.99	.88	5.61	1.26
white rice	4.98	.90	5.57	1.27
12.2% m.c.	4.95	.90	5.50	1.25
cv. 'Lebonnet'	4.91	.95	5.38	1.25
[46]	4.84	.93	4.22	1.16
	4.76	.88	5.03	1.04
	4.89	.89	5.10	1.01

Table 6.1c Continuation of Table 6.1. "B" = "Böttcher." "BH" = "Bruggeman-Hanai."

electric constant of an air-particle mixture with its density is consistent with the Landau and Lifshitz, Looyenga mixture equation (2).

$$(\epsilon')^{1/3} = \frac{(\epsilon_2')^{1/3} - 1}{\rho_2}\rho + 1 \tag{19}$$

6.4 Experimental Data

Data from several studies have been selected for inclusion here to compare solid material permittivities obtained by extrapolation of the linear functions with those predicted by the mixture equations. In addition, new measurements on solid samples and particulate samples of the same material are presented to assess better the reliability of both procedures for these particular materials.

a. Measurement Methods

The permittivities of all the materials included were measured at microwave frequencies by the short-circuited line or waveguide technique originally reported by Roberts and von Hippel [39], with computation by a general computer program described previously [40–41]. The measurement systems have also been described in detail previously for the 21 mm coaxial-line measurements [42] and for X-band [43–44] and K-band [44–45] rectangular waveguide measurements. Permittivity measurements on particulate materials at different densities were obtained by loosely filling sample holders, taking care to obtain plane sample-air interfaces perpendicular to the direction of wave propagation, and taking measurements before and after successive settling and compacting of the sample, with efforts to avoid nonuniform densities. Some samples were compressed (< 42 MPa) to relatively high volume fractions with a laboratory press [44], [46]. Particulate sample densities were calculated from sample weights and volumes determined from sample lengths in the sample holders during permittivity measurements. Solid sample densities were calculated from sample weights and volumes calculated from micrometer measurements of sample dimensions. Particle densities for materials for which solid samples were not available for permittivity measurements were determined from sample weights and volumes determined on particulate samples by air comparison pycnometer measurements.

b. Processing of Data for Extrapolation to Solid Density

The method of extrapolating from measurements on particulate material to obtain the permittivity of the solid material [6–7] will now be explained. A set of measurement data on ground rough rice [46] is selected for illustration, and a plot of the dielectric constant vs. bulk density is shown in Fig. 6.2. The point ($\rho = 0$, $\epsilon' = 1$) is included in

Material	Freq., GHz	Measured properties				Vol. frac.
		Density, g/cm^3		Permittivity, Particulate		
		Solid	Partic.			
		ρ_2	ρ	ϵ'	ϵ''	v_2
Illinois #6 run-of-mine [38, 49]	11.7	1.590	.604	2.01	.078	.380
			.657	2.13	.090	.413
			.677	2.16	.094	.426
			.705	2.24	.103	.443
			.733	2.29	.111	.461
			.760	2.35	.114	.478
			.801	2.44	.122	.504
			.837	2.52	.128	.526
			.866	2.60	.131	.545
			.894	2.69	.139	.562
Dahm run-of-mine [38]	11.7	2.020	.544	1.89	.051	.269
			.578	1.95	.052	.286
			.604	2.01	.059	.299
			.636	2.07	.066	.315
			.678	2.17	.080	.336
			.705	2.22	.081	.349
			.724	2.25	.085	.358
			.762	2.35	.088	.377
			.790	2.42	.092	.391
			.824	2.50	.099	.408

Table 6.2a Comparison of permittivities of solid coal estimated by extrapolation of linear density functions of the dielectric constant and loss factor with those predicted by indicated mixture equations from permittivity measurements on pulverized coal at 22° C. Tabular data rounded to one, two, three, or four decimal places. All calculations performed on unrounded data.

this data set, and a linear regression analysis provides the values of the regression constants A_0 and A_1 along with the regression coefficient and other statistics

$$\sqrt{\epsilon'} = A_0 + A_1\rho \tag{20}$$

A similar regression can be calculated for the cube root of ϵ'

$$(\epsilon')^{1/3} = A_0 + A_1\rho \tag{21}$$

where the regression coefficients will have different numerical values from those of (20). Inclusion of point $(0,1)$ in the regression calculation

Estimated complex permittivity of solid material						
Extrapolation of linear functions†			Mixture equations			
$(\epsilon')^{1/2}$	$(\epsilon')^{1/3}$	$(\epsilon''+\epsilon)^{1/2}$	RI		LLL	
ϵ'	ϵ'	ϵ''	ϵ'	ϵ''	ϵ'	ϵ''
4.50±.06	4.82±.05	.33±.02	4.42	.31	4.84	.37
			4.46	.32	4.86	.38
			4.44	.32	4.82	.38
			4.48	.33	4.82	.38
			4.47	.34	4.83	.40
			4.46	.33	4.81	.39
			4.47	.33	4.79	.38
			4.48	.33	4.79	.37
			4.50	.32	4.79	.36
			4.56	.32	4.86	.37
5.83±.11	6.58±.07	.49±.04	5.72	.33	6.63	.44
			5.70	.31	6.56	.41
			5.72	.33	6.57	.43
			5.74	.35	6.57	.45
			5.81	.39	6.62	.50
			5.56	.36	6.54	.48
			5.76	.38	6.52	.48
			5.82	.37	6.58	.46
			5.86	.37	6.60	.46
			5.86	.37	6.57	.46

Table 6.2b Continuation of Table 6.2. "RI" = "Refractive Index." "LLL" = "Landau & Lifshitz, Looyenga." †Calculated values with extrapolated 95% confidence intervals.

assures that the intercept A_0 will be essentially 1, and A_1 corresponds to the slope m of (18) or (19). (20) or (21) provide the estimate of ϵ' for the solid material when the density of the solid is known. These results are illustrated in Fig. 6.3 for both the square-root and cube-root cases. Also shown for comparison are the dashed regression lines that are obtained if the point $(0,1)$ is excluded from the regression analysis. In this instance, the cube-root plot generally results in an intercept closer to 1 than does the square-root plot, indicating that the cube root of ϵ' and density relationship may be closer to true linearity.

The plot of these data on ground rough rice for the loss factor is shown in Fig. 6.4 with a second-order polynomial regression curve

Material	Estimated complex permittivity of solid material			
	Mixture equations			
	B		BH	
	ϵ'	ϵ''	ϵ'	ϵ''
Illinois #6	4.98	.40	5.66	.58
run-of-mine	4.94	.39	5.60	.57
[38, 49]	4.87	.39	5.49	.56
	4.89	.39	5.52	.56
	4.84	.40	5.45	.56
	4.80	.38	5.39	.54
	4.76	.37	5.32	.51
	4.74	.36	5.28	.49
	4.73	.35	5.25	.47
	4.78	.35	5.30	.47
Dahm	7.66	.63	10.15	1.31
run-of-mine	7.43	.56	9.74	1.13
[38]	7.34	.57	9.60	1.15
	7.22	.57	9.40	1.14
	7.15	.60	9.30	1.19
	6.98	.56	8.99	1.08
	6.91	.55	8.86	1.06
	6.88	.51	8.81	.98
	6.84	.50	8.74	.95
	6.74	.49	8.54	.91

Table 6.2c Continuation of Table 6.2. "B" = "Böttcher." "BH" = "Bruggeman-Hanai."

fitted to the data, which included the $(0,0)$ point in the calculation.

$$\epsilon'' = A_0 + A_1\rho + A_2\rho^2 \tag{22}$$

Inclusion of the point $(0,0)$ in the data set assures that A_0 will be negligibly small, and thus (22) provides the values for the constants c and d of (14), $A_2 = c$, $A_1 = d$. By (17), e is determined, and the linear regression calculation corresponding to (16) can be completed,

$$\sqrt{\epsilon'' + e} = A_0 + A_1\rho \tag{23}$$

which then permits the linear extrapolation to the density of the solid material to estimate its loss factor as illustrated in Fig. 6.5.

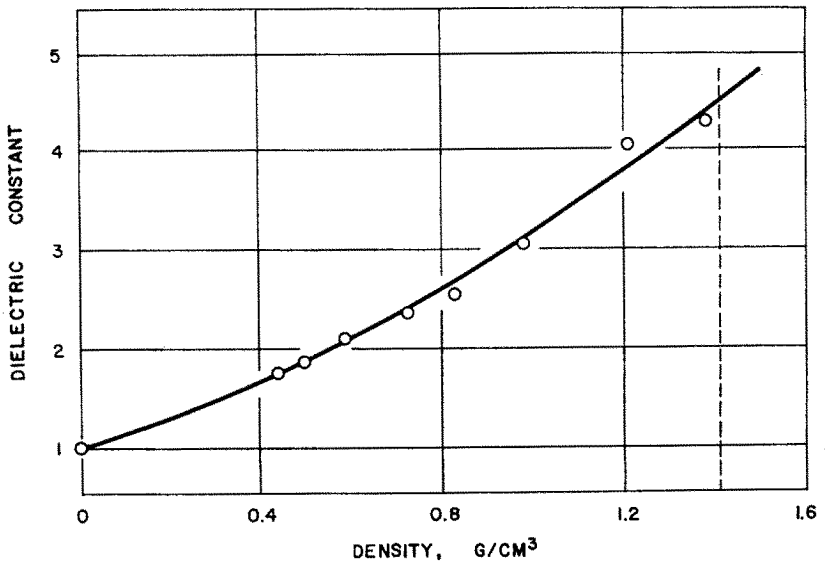

Figure 6.2 Density dependence of the dielectric constant of ground 'Brazos' rough rice of 11.5% moisture content at 11.0 GHz and 24° C [46].

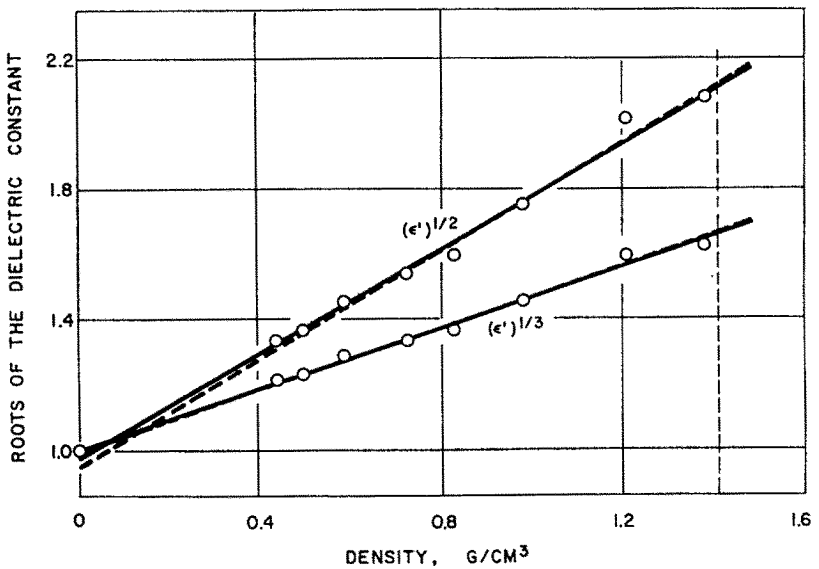

Figure 6.3 Linear regressions of the square and cube roots of the dielectric constant ϵ' of ground 'Brazos' rough rice of 11.5% moisture content on bulk density at 11.0 GHz and 24° C [46].

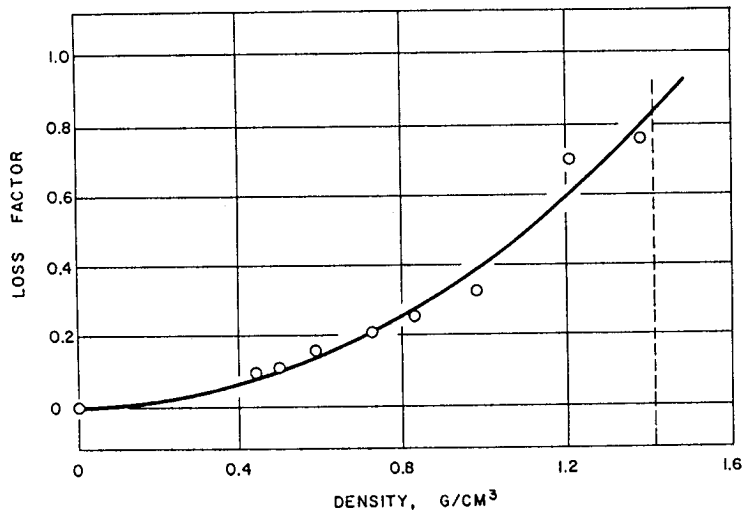

Figure 6.4 Quadratic dependence of the loss factor of ground 'Brazos' rough rice of 11.5% moisture content on bulk density at 11.0 GHz and 24° C [46].

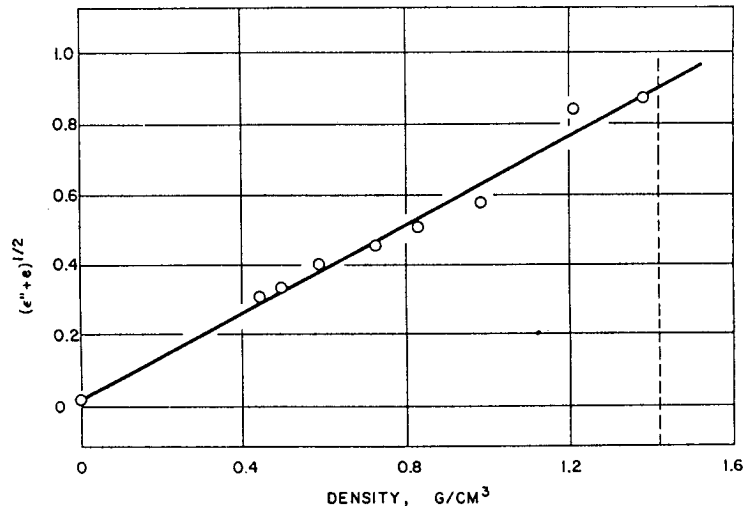

Figure 6.5 Linear regression of the function of the loss factor ϵ'' of ground 'Brazos' rough rice of 11.5% moisture content on bulk density at 11.0 GHz and 24° C, with extrapolation to determine ϵ'' of the kernel at kernel density of 1.409 g/cm^3 [46].

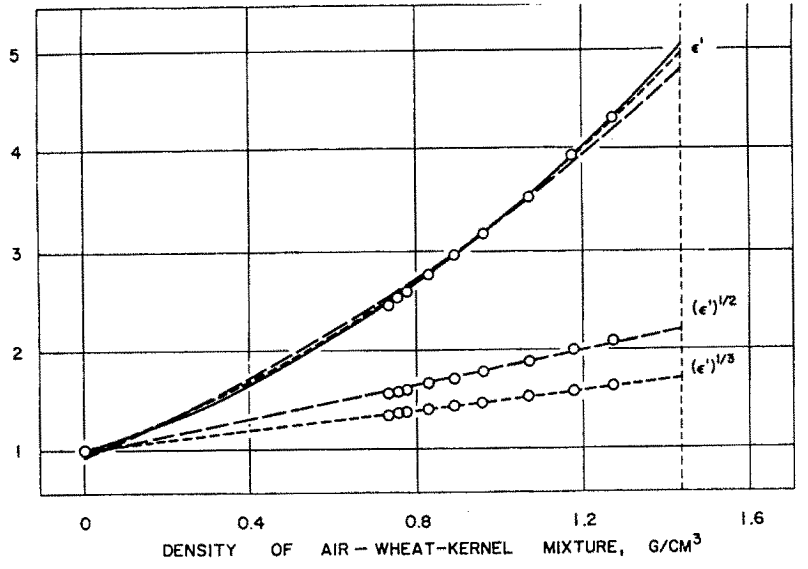

Figure 6.6 Comparison of measured dielectric constant ϵ' values of 'Scout 66' whole-kernel, hard red winter wheat of 11.5% moisture content at 9.4 GHz and 24° C with those predicted by linear regression of $(\epsilon')^{1/2}$ and $(\epsilon')^{1/3}$ on bulk density. Solid curve for ϵ' determined by second-order polynomial regression. Long-dashed and short-dashed curves for ϵ' obtained from corresponding linear regressions [30].

6.5 Examples of Applications

Other examples [30] comparing estimated values for the dielectric constant are shown in Figs. 6.6, 6.7, and 6.8 for whole-kernel hard red winter wheat, ground wheat, and pulverized coal. Plots of the square and cube roots of the measured dielectric constants are shown along with the curves for ϵ' predicted from these linear relationships with density. The solid curves for ϵ' are second-order regression curves fitted to the data, but outside the range of measurements, the values on these solid-lines are not necessarily the correct values. The ϵ' values predicted by the cube-root relationship are consistently higher than those predicted by the square-root relationship, but, unfortunately, for these materials the correct values for the solid material are not known.

The ϵ' values predicted by the square-root and cube-root relationships from these experimental data were compared within the density range where permittivities were measured [30], and they predicted ϵ' to within 4% and 2%, respectively, for whole-kernel wheat. For ground

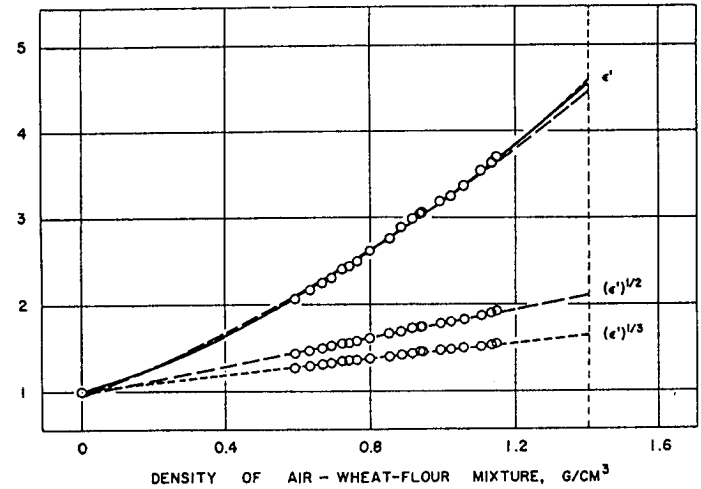

Figure 6.7 Comparison of measured dielectric constant ϵ' values of ground 'Scoutland' hard red winter wheat of 10.9% moisture content at 11.7 GHz and 22° C with those predicted by linear regression of $(\epsilon')^{1/2}$ and $(\epsilon')^{1/3}$ on bulk density. Solid curve for ϵ' determined by second-order polynomial regression. Long-dashed and short-dashed curves for ϵ' obtained from corresponding linear regressions [30].

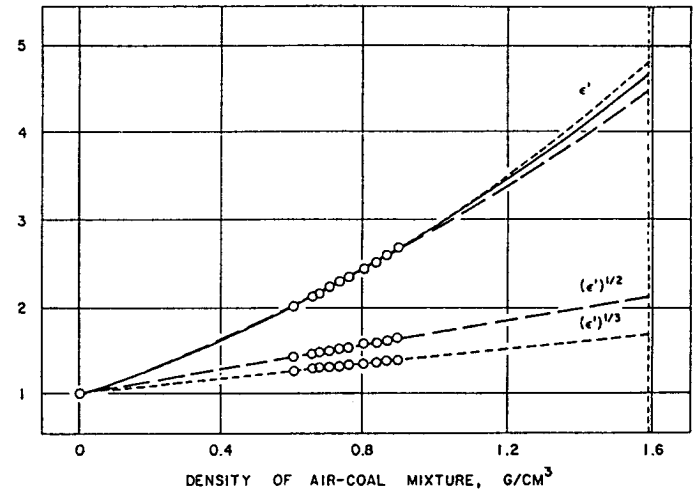

Figure 6.8 Comparison of measured dielectric constant ϵ' values of dry, pulverized Illinois No. 6 run-of-mine coal at 11.7 GHz and 22° C with those predicted by linear regression of $(\epsilon')^{1/2}$ and $(\epsilon')^{1/3}$ on bulk density. Solid curve for ϵ' determined by second-order polynomial regression. Long-dashed and short-dashed curves for ϵ' obtained from corresponding linear regressions [30].

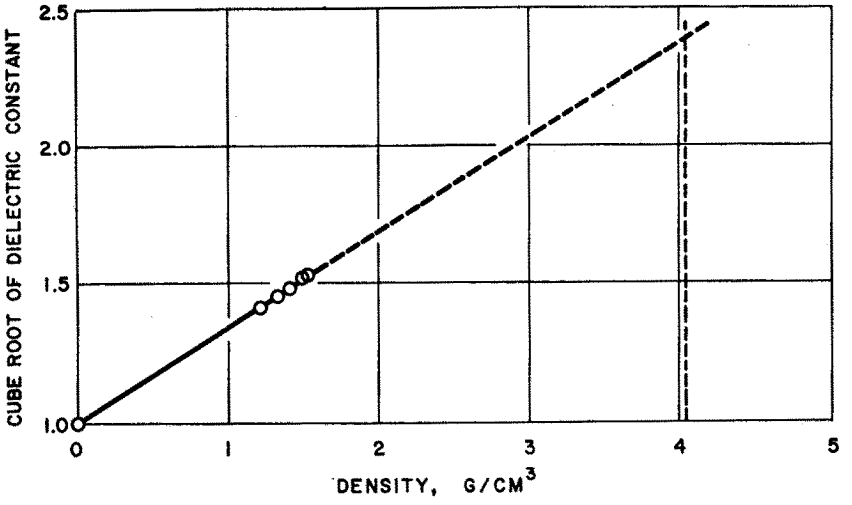

Figure 6.9 Linear extrapolation of the cube root of the dielectric constant ϵ' of dry, pulverized goethite to determine ϵ' for solid goethite at 11.7 GHz and 24° C at the density of the solid material (4.04 g/cm^3) [6,7].

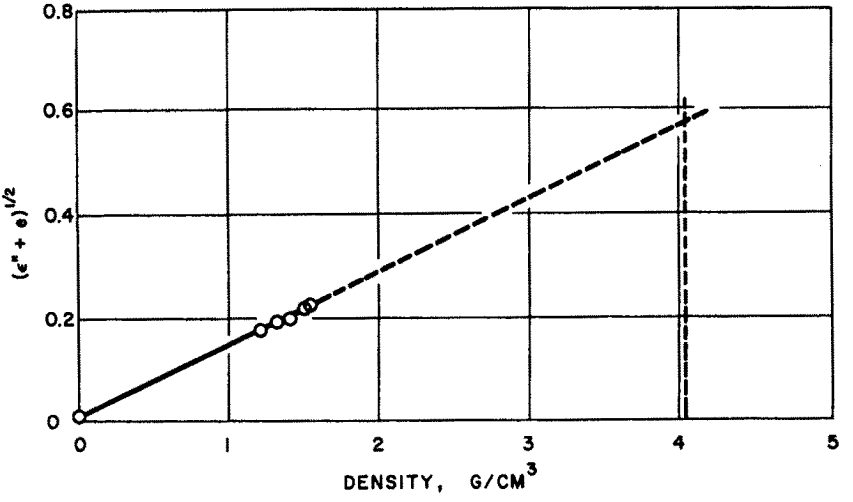

Figure 6.10 Linear extrapolation of the function of the loss factor ϵ'' of dry pulverized goethite to determine ϵ'' for solid goethite at 11.7 GHz and 24° C at the density of the solid materials (4.04 g/cm^3) [6,7].

Material	Freq., GHz	Measured properties				Vol. frac.
		Density, g/cm^3		Permittivity, Particulate		
		Solid	Partic.			
		ρ_2	ρ	ϵ'	ϵ''	v_2
Chlorite (clinochlore) [47]	22.0	2.76	.693	1.85	.014	.251
			.742	1.93	.014	.269
			.790	2.02	.018	.286
			.849	2.10	.020	.308
			.887	2.16	.022	.321
			.999	2.32	.028	.362
Feldspar (labradorite) [47]	22.0	2.72	.953	2.14	.0073	.350
			1.044	2.29	.0087	.384
			1.191	2.52	.0128	.438
			1.355	2.78	.0147	.498
			1.462	2.99	.0157	.538
Mica (phlogopite) [47]	22.0	2.96	.508	1.73	.012	.172
			.556	1.79	.014	.188
			.606	1.86	.014	.205
			.662	1.97	.014	.224
			.739	2.10	.017	.250
			.838	2.30	.022	.283
Goethite [47]	11.7	4.04	1.227	2.84	.032	.304
			1.334	3.05	.036	.330
			1.424	3.25	.040	.352
			1.511	3.49	.049	.374
			1.555	3.59	.051	.385

Table 6.3a Comparison of permittivities of selected minerals estimated by extrapolation of linear density functions of the dielectric constant and loss factor with those predicted by indicated mixture equations from permittivity measurements on pulverized coal at 24° C. Tabular data rounded to one, two, three, or four decimal places. All calculations performed on unrounded data.

wheat, the corresponding errors of prediction were 2% and 0.5%, and for the finely pulverized coal they were 1% and 0.1%, indicating that the error of prediction is correlated with particle size. The wheat kernels had a mean length of 6.7 mm and mean diameter of 2.7 mm. The ground wheat had about 25% of its particles smaller than 250 μm and nearly all of the remainder ranged between 250 and 1000 μm, whereas the pulverized coal particles were all smaller than 250 μm with 70 percent of the particles smaller than 90 μm.

Estimated complex permittivity of solid material								
Extrapolation of linear functions†			Mixture equations					
$(\epsilon')^{1/2}$	$(\epsilon')^{1/3}$	$(\epsilon''+\epsilon)^{1/2}$	RI		LLL		B	
ϵ'	ϵ'	ϵ''	ϵ'	ϵ''	ϵ'	ϵ''	ϵ'	ϵ''
6.02±.09	6.92±.19	.212±.018	5.96	.10	6.97	.13	8.42	.21
			6.01	.09	7.01	.12	8.25	.18
			6.10	.11	7.09	.14	8.17	.20
			6.02	.11	6.94	.15	7.76	.19
			6.05	.12	6.96	.15	7.67	.19
			6.00	.11	6.82	.16	7.23	.18
5.50±.12	6.03±.11	.050±.009	5.40	.033	6.09	.042	6.45	.048
			5.46	.034	6.11	.044	6.33	.047
			5.48	.043	6.06	.053	6.12	.053
			4.48	.041	5.98	.049	5.92	.048
			5.55	.040	6.02	.047	5.90	.044
7.89±.27	9.63±.45	.116±.025	8.08	.15	10.23	.23	21.36	1.18
			7.81	.15	9.77	.22	17.39	.82
			7.75	.14	9.61	.20	15.50	.60
			7.81	.12	9.64	.18	14.41	.43
			7.78	.13	9.50	.18	12.93	.36
			8.00	.14	9.70	.20	12.20	.33
10.89±.51	13.39±.34	.327±.028	10.58	.20	13.27	.30	17.35	.51
			10.64	.21	13.22	.29	16.02	.43
			10.76	.21	13.26	.29	15.27	.38
			11.02	.23	13.50	.32	14.92	.39
			11.06	.23	13.49	.32	14.62	.37

Table 6.3b Continuation of Table 6.3. "RI" = "Refractive Index." "LLL" = "Landau & Lifshitz, Looyenga." "B" = "Böttcher." †Calculated values with extrapolated 95% confidence intervals.

These extrapolation procedures were also applied to measurements on pulverized and purified minerals for which no information on the permittivities of the solid materials is available. Mineral samples are described elsewhere [47]. In this instance the cube-root relationship was applied for ϵ', because it appeared to have better precision of prediction within the density range of measured permittivities. Typical results are illustrated graphically in Figs. 6.9 and 6.10. Both square-root and cube-root extrapolations for ϵ' were used in the development of models for the dielectric constants of several cereal grains and soybeans as functions of density, frequency, and moisture content [48].

Freq., GHz	Measured properties				Vol. frac.
	Density, g/cm^3		Permittivity, Particulate		
	Solid	Partic.			
	ρ_2	ρ	ϵ'	ϵ''	v_2
1.0	4.75	2.277	8.37	1.81	.479
		2.408	8.84	1.87	.507
		2.527	10.36	2.58	.532
		2.628	11.42	3.02	.553
		2.690	11.98	3.29	.566
2.45		2.277	6.56	1.64	.479
		2.408	6.80	2.58	.507
		2.527	8.27	2.76	.532
		2.628	8.16	3.41	.553
		2.690	8.91	3.71	.566
5.5		2.179	5.77	1.51	.459
		2.327	6.12	1.50	.490
		2.512	6.87	1.70	.529
		2.607	7.38	1.98	.549
		2.675	7.62	2.10	.563
11.7		2.011	4.58	.49	.423
		2.127	5.19	.68	.448
		2.257	5.63	.82	.475
		2.424	6.27	1.02	.510
		2.539	6.71	1.21	.535
		2.642	7.30	1.25	.556
22.0		1.862	4.23	.23	.392
		1.942	4.68	.08	.409
		2.410	4.72	.45	.507
		2.513	4.78	.53	.529
		2.593	5.23	.55	.546

Table 6.4a Comparison of permittivities of the mineral ilmenite estimated by extrapolation of linear density functions of the dielectric constant and loss factor [47] with those predicted by indicated mixture equations from permittivity measurements on pulverized samples at 24° C. Tabular data rounded to one, two, three, or four decimal places. All calculations performed on unrounded data.

Estimated complex permittivity of solid material								
Extrapolation of linear functions†			Mixture equations					
$(\epsilon')^{1/2}$	$(\epsilon')^{1/3}$	$(\epsilon''+\epsilon)^{1/2}$	RI		LLL		B	
ϵ'	ϵ'	ϵ''	ϵ'	ϵ''	ϵ'	ϵ''	ϵ'	ϵ''
26.8±4.8	33.3±5.1	7.6±2.4	24.4	6.5	31.0	9.1	29.0	7.9
			23.9	6.1	29.8	8.3	27.1	6.9
			26.6	7.8	33.1	10.6	29.3	8.5
			26.0	8.6	34.5	11.5	30.1	9.0
			26.5	9.0	34.9	11.9	30.2	9.3
19.2±3.1	23.2±3.5	8.5±2.8	16.0	8.2	22.2	7.6	21.2	7.0
			17.2	8.2	20.6	10.9	19.5	9.4
			20.4	8.2	24.6	10.9	22.4	9.0
			20.4	8.2	22.2	12.3	20.4	10.1
			20.2	9.9	23.8	12.8	21.6	10.4
16.7±0.9	20.0±0.7	5.9±0.8	16.3	5.6	20.0	7.6	19.7	7.2
			16.0	5.0	19.3	6.7	18.4	5.9
			16.5	5.0	19.6	6.5	18.2	5.5
			16.9	5.5	20.0	7.1	18.4	5.9
			17.0	5.6	19.9	7.1	18.2	5.9
15.6±1.9	18.7±1.7	3.1±0.9	13.7	2.0	16.8	2.7	17.3	2.8
			14.8	2.5	18.2	3.5	18.1	3.4
			15.1	2.8	18.3	3.8	17.7	3.5
			15.6	3.2	18.6	4.1	17.5	3.6
			15.7	3.5	18.7	4.5	17.2	3.8
			16.5	3.4	19.4	4.3	17.7	3.6
11.4±4.0	13.2±5.4	1.3±0.9	13.7	1.0	17.1	1.5	16.5	1.7
			14.8	.4	18.5	.5	18.5	.5
			11.0	1.4	12.7	1.7	12.2	1.6
			10.5	1.5	12.0	1.8	11.5	1.6
			11.2	1.5	13.0	1.9	12.2	1.6

Table 6.4b Continuation of Table 6.4. "RI" = "Refractive Index." "LLL" = "Landau & Lifshitz, Looyenga." "B" = "Böttcher." †Calculated values with extrapolated 95% confidence intervals.

Grain	Particle size*, μm					
	>1000	1000	500	250	125	63
Wheat, hard red winter, 10.9% m.c., cv. 'Scout 66'	0.7	46.3	28.4	13.9	6.2	4.5
Rice, white (milled) 11.2% m.c., cv. 'Lebonnet'	0.2	62.3	24.0	10.4	2.7	0.5

*Column heading is particle size upper limit; lower limit is heading of next column; last column includes all particles smaller than 63 μm.

Table 6.5 Particle-size distribution for ground grain (% by weight).

Coal	Particle size*, μm						
	>250	250	180	125	90	63	45
Illinois #66, run-of-mine [49]	3.2	7.8	12.7	12.0	17.8	15.5	31.0
Dahm, run-of-mine [38]	1.0	4.8	10.0	15.8	31.2	23.6	13.6

*Column heading is particle size upper limit; lower limit is heading of next column; last column includes all particles smaller than 45 μm.

Table 6.6 Particle-size distribution for pulverized coal (% by weight).

Mineral	Particle size*, μm												
	176	125	88	62	44	31	22	16	11	7.8	5.5	3.9	2.8
Chlorite (clinochlore)	9.3	22.7	21.2	10.7	11.8	7.9	2.9	5.3	1.6	2.4	2.0	0.9	0.9
Feldspar (labradorite)	2.3	14.4	17.4	15.9	13.5	10.2	6.7	6.4	3.1	2.3	3.1	1.9	2.4
Mica (phlogopite)	1.9	17.4	22.6	15.4	17.6	9.3	1.9	5.8	3.1	1.8	1.4	0.9	0.5
Goethite	0.4	7.9	12.2	15.6	17.9	13.2	10.2	8.3	5.9	3.5	2.2	1.3	0.7
Ilmenite	0.9	14.6	26.0	15.1	11.6	8.9	5.2	4.8	3.9	3.0	2.0	2.2	1.2

*Column heading is particle size upper limit; lower limit is heading of next column; last column includes all particles smaller than 2.8 μm.

Table 6.7 Particle-size distribution for pulverized mineral samples (% by weight).

6.6 Comparison of Extrapolation and Mixture Equation Predictions

a. General Comparisons

Permittivity measurements on several kinds of particulate materials were selected for comparison of extrapolation predictions of solid permittivities with those predicted by the mixture equations. Pertinent data for comparisons on whole-kernel wheat, ground wheat, and

ground white rice are presented in Table 6.1. The moisture content of the grain in percent, wet basis, and the grain cultivar are listed, along with references to original publications. Included also are the frequency at which measurements were made, the density of the solid material, and the densities and corresponding permittivities of the air-particle mixtures over a series of densities. Next are listed the permittivity values obtained by extrapolation and the permittivities predicted by complex algebraic calculation from the indicated mixture equations. In each case, the cube-root extrapolation predicts a higher value for ϵ' of the kernels than the square-root relationship; however, when the statistical uncertainty of the extrapolation is taken into account, as indicated by the extrapolated 95% confidence intervals, the ranges of these two extrapolated values overlap. The range of ϵ' values given by the Refractive Index equation over the range of densities and volume fractions includes the value obtained by the square-root extrapolation, since they are consistent relationships. Likewise the range of ϵ' values provided by the Landau and Lifshitz, Looyenga equation includes the value obtained by the cube-root extrapolation, since they are also consistent relationships. Values for ϵ' predicted by the Böttcher equation are very close to those of the Landau and Lifshitz, Looyenga equation. For these particulate materials at the measured volume fractions, the Bruggeman-Hanai equation gives ϵ' values considerably greater than the other equations. The Lichtenecker and Rayleigh equations gave values for ϵ' even larger, so those results are not listed.

Values for ϵ' provided by the various mixture equations depend upon the density or volume fraction at which the samples were measured, increasing with increasing volume fraction for most of the data in Table 6.1, except for the Böttcher and Bruggeman-Hanai equations. Dielectric constants given by the Bruggeman-Hanai equation tend to decrease, coming closer to the probable true value, with higher volume fractions. Values given by the Böttcher equation vary less over the density range, increasing with volume fraction for whole-wheat kernels, decreasing for ground white rice, and remaining nearly constant for the ground wheat.

Loss-factor values predicted for the solid materials (kernels) by the Refractive Index equation are somewhat smaller than the values obtained by extrapolation. Values of ϵ'' from the Landau and Lifshitz, Looyenga equation include the extrapolated values within their range. Loss factors from the Böttcher equation tend to be a little lower

Freq., GHz	Measured properties						Vol. frac.
	Density, g/cm^3		Permittivity,				
	Solid	Partic.	Solid		Particulate		
	ρ_2	ρ	ϵ'	ϵ''	ϵ'	ϵ''	v_2
2.45	1.049	.442	2.532	.0027	1.54	.0005	.421
		.456			1.56	.0009	.435
		.467			1.58	.0010	.445
		.497			1.62	.0009	.474
		.521			1.66	.0012	.497
		.526			1.66	.0008	.501
		.533			1.68	.0008	.508
		.539			1.69	.0011	.514
		.544			1.70	.0009	.519
11.5	1.049	.423	2.53	.003	1.51	.0005	.403
		.453			1.54	.0005	.432
		.480			1.57	.0007	.458
		.503			1.60	.0007	.480
		.538			1.67	.0007	.513
		.589			1.75	.0009	.562
		.645			1.84	.0014	.615
		.707			1.93	.0015	.674
		.762			2.00	.0021	.727
22.0	1.049	.374	2.53	.014	1.43	.0018	.357
		.401			1.47	.0020	.382
		.447			1.53	.0003	.426
		.492			1.59	.0011	.469
		.569			1.71	.0052	.542
		.670			1.87	.0039	.639
		.815			2.07	.0063	.777
		.910			2.23	.0152	.868
		.958			2.32	.0177	.913

Table 6.8a Comparison of permittivity values for Rexolite 1422 estimated for solid material from measurements at 25° C on a particulate sample by extrapolation of linear density functions of the dielectric constant and loss factor and by indicated dielectric mixture equations. Tabular data rounded to one, two, three, or four decimal places. All calculations performed on unrounded data.

Estimated complex permittivity of solid material						
Extrapolation of linear functions†			Mixture equations			
$(\epsilon')^{1/2}$	$(\epsilon')^{1/3}$	$(\epsilon''+\epsilon)^{1/2}$	RI		LLL	
ϵ'	ϵ'	ϵ''	ϵ'	ϵ''	ϵ'	ϵ''
2.50±.02	2.57±.02	.0024±.0010	2.48	.0015	2.56	.0017
			2.48	.0027	2.57	.0029
			2.49	.0027	2.57	.0030
			2.49	.0024	2.56	.0026
			2.49	.0031	2.57	.0034
			2.49	.0020	2.57	.0021
			2.50	.0020	2.58	.0022
			2.51	.0026	2.58	.0029
			2.51	.0020	2.58	.0022
2.47±.05	2.52±.04	.0030±.0007	2.45	.0015	2.54	.0017
			2.44	.0015	2.52	.0017
			2.41	.0018	2.48	.0020
			2.42	.0019	2.49	.0021
			2.45	.0017	2.52	.0019
			2.48	.0019	2.54	.0020
			2.49	.0027	2.54	.0029
			2.48	.0026	2.53	.0027
			2.46	.0032	2.50	.0034
2.46±.03	2.49±.03	.016±.012	2.41	.0066	2.49	.0073
			2.44	.0069	2.52	.0076
			2.43	.0010	2.51	.0011
			2.43	.0030	2.50	.0033
			2.46	.0116	2.52	.0125
			2.48	.0070	2.53	.0074
			2.45	.0088	2.48	.0091
			2.46	.0184	2.48	.0187
			2.47	.0200	2.48	.0202

Table 6.8b Continuation of Table 6.8. "RI" = "Refractive Index." "LLL" = "Landau & Lifshitz, Looyenga." †Calculated values with extrapolated 95% confidence intervals.

Freq., GHz	Estimated complex permittivity of solid material							
	Mixture equations							
	B		BH		R		L	
	ϵ'	ϵ''	ϵ'	ϵ''	ϵ'	ϵ''	ϵ'	ϵ''
2.45	2.57	.0017	2.63	.0019	2.71	.0021	2.79	.0022
	2.57	.0030	2.64	.0033	2.71	.0037	2.79	.0038
	2.58	.0030	2.64	.0034	2.72	.0038	2.80	.0039
	2.56	.0026	2.63	.0028	2.70	.0032	2.77	.0032
	2.56	.0034	2.63	.0037	2.70	.0042	2.77	.0042
	2.56	.0021	2.62	.0023	2.70	.0026	2.76	.0027
	2.57	.0021	2.64	.0023	2.71	.0026	2.77	.0027
	2.58	.0028	2.64	.0031	2.71	.0035	2.77	.0035
	2.58	.0022	2.64	.0024	2.72	.0027	2.78	.0027
11.5	2.55	.0017	2.61	.0019	2.68	.0021	2.77	.0022
	2.52	.0017	2.58	.0018	2.65	.0021	2.73	.0021
	2.49	.0020	2.54	.0022	2.61	.0025	2.68	.0025
	2.49	.0021	2.54	.0023	2.61	.0025	2.68	.0026
	2.52	.0019	2.57	.0020	2.64	.0023	2.70	.0023
	2.53	.0020	2.59	.0022	2.66	.0024	2.71	.0024
	2.53	.0028	2.58	.0031	2.64	.0034	2.68	.0034
	2.51	.0026	2.56	.0028	2.62	.0031	2.64	.0031
	2.49	.0033	2.53	.0035	2.57	.0038	2.60	.0038
22.0	2.52	.0076	2.57	.0083	2.63	.0092	2.73	.0097
	2.54	.0078	2.60	.0086	2.67	.0096	2.76	.0100
	2.52	.0011	2.57	.0012	2.64	.0014	2.72	.0014
	2.50	.0033	2.56	.0036	2.62	.0040	2.69	.0041
	2.51	.0124	2.57	.0135	2.64	.0151	2.69	.0152
	2.52	.0073	2.57	.0079	2.63	.0087	2.66	.0087
	2.47	.0089	2.50	.0094	2.63	.0087	2.56	.0100
	2.46	.0185	2.48	.0190	2.51	.0199	2.52	.0197
	2.48	.0202	2.49	.0205	2.51	.0211	2.51	.0210

Table 6.8c Continuation of Table 6.8. "B" = "Böttcher." "BH" = "Bruggeman-Hanai." "R" = "Rayleigh." "L" = "Lichtenecker."

than those of the Landau and Lifshitz, Looyenga equation, and the Bruggeman-Hanai equation gives loss factors generally a little above the extrapolated values.

A similar tabulation of data for two pulverized coal samples (Table 6.2) shows the same type of agreement between the Refractive Index equation and extrapolated ϵ' from the square-root relationship and between the Landau and Lifshitz, Looyenga equation and the cube-root extrapolation. Values of ϵ' given by the Landau and Lifshitz, Looyenga equation are relatively independent of volume fraction, whereas the Böttcher and Bruggeman-Hanai equations show more variation with volume fraction for these finely pulverized samples. The Lichtenecker and Rayleigh equations predicted even larger permittivity values.

The Refractive Index equation gave loss factors agreeing very well with the extrapolated value for the Illinois #6 coal sample, but the extrapolated ϵ'' value for the Dahm coal sample was high, relative to the values given by this mixture equation. In this instance, the extrapolated ϵ'' value agreed better with the Landau and Lifshitz, Looyenga equation. The Böttcher and Bruggeman-Hanai equations gave somewhat higher loss factors.

Comparison data for four pulverized mineral samples [47] are summarized in Table 6.3. The three silicates, chlorite, feldspar, and mica, were measured at 22 GHz, and the metal hydroxide, goethite, was measured at 11.7 GHz. As expected, the square-root extrapolations for ϵ' of the solid material agree well with the Refractive Index mixture equation predictions, and the cube-root extrapolations agree with the Landau and Lifshitz, Looyenga equation predictions. The Böttcher equation provides ϵ' values considerably greater than the other equations. The Bruggeman-Hanai, Lichtenecker, and Rayleigh equations gave such high values that they are not listed. Except for the Böttcher equation, variation in predicted ϵ' values with volume fraction was relatively low; however, the goethite showed more variation in this respect than did the silicates. Except for the mica sample, the extrapolated values for ϵ'' were higher than the values predicted by the Refractive Index equation. The loss factors predicted by the Landau and Lifshitz, Looyenga equation agreed better with the extrapolated ϵ'' values.

Measurements and calculations on a pulverized metal oxide mineral of high permittivity, ilmenite, over the frequency range from 1 to 22 GHz are summarized in Table 6.4. Again, the square-root and cube-root extrapolated values for ϵ' are included in the range of values

Freq., GHz	Measured properties						Vol. frac.
	Density, g/cm^3		Permittivity,				
	Solid	Partic.	Solid		Particulate		
	ρ_2	ρ	ϵ'	ϵ''	ϵ'	ϵ''	v_2
2.45	1.767	.467	2.828	.223	1.40	.037	.264
		.488			1.43	.041	.276
		.506			1.45	.044	.286
		.522			1.46	.044	.295
		.592			1.54	.053	.335
		.638			1.56	.057	.361
		.698			1.64	.062	.395
		.763			1.71	.076	.432
		.794			1.75	.079	.449
11.5	1.767	.486	2.689	.100	1.37	.022	.275
		.522			1.39	.021	.295
		.570			1.45	.022	.322
		.645			1.55	.027	.365
		.676			1.59	.030	.382
		.714			1.64	.034	.404
		.860			1.78	.051	.486
		1.071			1.98	.064	.605
		1.252			2.18	.078	.709
22.0	1.767	.397	2.61	.12	1.31	.013	.225
		.470			1.39	.031	.266
		.533			1.45	.040	.302
		.595			1.48	.047	.337
		.677			1.56	.040	.383
		.781			1.66	.049	.442
		1.034			1.88	.095	.585
		1.295			2.20	.087	.733
		1.455			2.38	.097	.823

Table 6.9a Comparison of permittivity values for Kynar (polyvinylidene flouride) estimated for solid material from measurements at 25° C on a particulate sample by extrapolation of linear density functions of the dielectric constant and loss factor and by indicated dielectric mixture equations. Tabular data rounded to one, two, three, or four decimal places. All calculations performed on unrounded data.

Estimated complex permittivity of solid material						
Extrapolation of linear functions†			Mixture equations			
$(\epsilon')^{1/2}$	$(\epsilon')^{1/3}$	$(\epsilon''+\epsilon)^{1/2}$	RI		LLL	
ϵ'	ϵ'	ϵ''	ϵ'	ϵ''	ϵ'	ϵ''
2.94±.06	3.08±.05	.266±.014	2.85	.20	3.02	.24
			2.91	.21	3.08	.25
			2.94	.22	3.11	.25
			2.91	.21	3.02	.24
			2.94	.22	3.11	.25
			2.86	.22	3.01	.25
			2.93	.21	3.08	.24
			2.94	.23	3.07	.26
			2.95	.23	3.09	.26
2.81±.09	2.86±.11	.138±.014	2.64	.11	2.78	.13
			2.60	.10	2.72	.11
			2.66	.09	2.78	.10
			2.78	.10	2.91	.11
			2.82	.10	3.00	.13
			2.87	.11	2.93	.12
			2.84	.13	2.95	.15
			2.80	.13	2.87	.14
			2.79	.13	2.85	.13
2.74±.05	2.79±.06	.130±.040	2.71	.08	2.87	.10
			2.78	.16	2.94	.19
			2.80	.18	2.96	.21
			2.71	.19	2.84	.22
			2.72	.14	2.84	.16
			2.73	.14	2.84	.16
			2.67	.19	2.75	.21
			2.76	.13	2.81	.14
			2.76	.13	2.79	.13

Table 6.9b Continuation of Table 6.9. "RI" = "Refractive Index." "LLL" = "Landau & Lifshitz, Looyenga." †Calculated values with extrapolated 95% confidence intervals.

Freq., GHz	Estimated complex permittivity of solid material							
	Mixture equations							
	B		BH		R		L	
	ϵ'	ϵ''	ϵ'	ϵ''	ϵ'	ϵ''	ϵ'	ϵ''
2.45	3.12	.26	3.23	.30	3.36	.35	3.54	.36
	3.17	.28	3.30	.32	3.45	.38	3.61	.38
	3.20	.28	3.33	.33	3.49	.39	3.65	.38
	3.17	.27	3.29	.31	3.45	.37	3.60	.37
	3.17	.27	3.30	.32	3.47	.38	3.60	.37
	3.05	.26	3.17	.30	3.32	.35	3.43	.35
	3.11	.25	3.24	.29	3.40	.35	3.50	.34
	3.09	.26	3.21	.31	3.38	.37	3.46	.35
	3.10	.26	3.22	.30	3.39	.37	3.47	.35
11.5	2.84	.14	2.92	.16	3.02	.16	3.17	.18
	2.78	.12	2.85	.13	2.94	.15	3.08	.16
	2.83	.11	2.91	.13	3.02	.14	3.14	.15
	2.95	.12	3.05	.13	3.18	.16	3.30	.16
	2.98	.12	3.10	.14	3.24	.17	3.34	.16
	3.03	.13	3.15	.15	3.30	.18	3.40	.17
	2.95	.15	3.06	.17	3.20	.20	3.26	.19
	2.86	.13	2.94	.15	3.05	.17	3.08	.17
	2.83	.13	2.89	.14	2.98	.16	3.00	.15
22.0	2.97	.11	3.07	.12	3.16	.14	3.34	.15
	2.70	.10	3.12	.24	3.35	.28	3.41	.29
	3.02	.23	3.13	.26	3.26	.31	3.40	.31
	2.89	.23	2.97	.26	3.08	.30	3.21	.30
	2.87	.16	2.96	.18	3.08	.21	3.19	.21
	2.84	.16	2.94	.18	3.06	.21	3.14	.21
	2.73	.20	2.80	.23	2.90	.26	2.94	.25
	2.78	.14	2.84	.15	2.92	.16	2.94	.16
	2.77	.13	2.81	.13	2.87	.14	2.87	.14

Table 6.9c Continuation of Table 6.9. "B" = "Böttcher." "BH" = "Bruggeman-Hanai." "R" = "Rayleigh." "L" = "Lichtenecker."

Material	Particle size*, μm												
	176.0	125.0	88.0	62.0	44.0	31.0	22.0	16.0	11.0	7.8	5.5	3.9	2.8
Rexolite	16.9	26.2	19.3	13.5	7.0	3.1	3.3	2.4	1.3	4.1	0.5	0.0	2.4
Kynar (PVF)	17.3	26.6	14.0	10.1	3.9	4.7	3.3	3.3	7.9	3.5	2.0	1.6	1.8

*Column heading is particle size upper limit; lower limit is heading of next column; last column includes all particles smaller than 2.8 μm.

Table 6.10 Particle-size distribution for ground Rexolite 1422 and Kynar (PVF) samples (% by weight).

predicted by the Refractive Index and Landau and Lifshitz, Looyenga equations, respectively. The 95% confidence intervals are rather wide for these data on only five densities extrapolated far outside the range of measurement. In this instance, for ilmenite, the Böttcher equation most often gave ϵ' values a little lower than the Landau and Lifshitz, Looyenga equation, except at the lowest volume fraction measurement at 11.7 and 22.0 GHz. Again, the Bruggeman-Hanai, Lichtenecker, and Rayleigh equations were inappropriate, and results of those calculations are not listed.

Even though the variation in volume fraction was over rather narrow ranges, the ϵ' values predicted by most of the mixture equations showed some dependence on the volume fraction, tending to increase with volume fraction except at 22 GHz, where the opposite tendency is noted. The Böttcher equation showed less of this dependence on volume fraction except at 22 GHz.

For the loss factor, all three mixture equations gave values reasonably close to those obtained by extrapolation, but the Landau and Lifshitz, Looyenga equation generally gave higher values.

b. Particle Size and Shape Variation

Some of the differences noted in the prediction patterns of the different mixture equations may be attributable to differences in particle shapes and particle size distributions for the various materials represented in Tables 6.1 through 6.4. Therefore, particle size information is presented in Tables 6.5, 6.6 and 6.7. The whole-kernel wheat of Table 6.1 had the following mean kernel dimensions and standard deviations: length $= 6.69 \pm 0.44$ mm, narrow width $= 2.65 \pm 0.31$ mm, greater width $= 2.72 \pm 0.19$ mm. These are by far the largest particles of all the particulate materials represented here. Their large size may account for the somewhat greater dependence of the ϵ' values predicted

by the mixture equations on the variation in volume fraction for the materials in Table 6.1. All three materials in Table 6.1 had a similar range of volume fractions which varied from loosely filled to compressed pellets that retained their form when removed from the sample holder. The somewhat lesser dependence of the predicted ϵ' values for ground rice on volume fraction, compared to the ground whole wheat, may have resulted from the more uniform particle size and lesser variation in structure and composition of the particles of the ground white rice sample, because it contained no bran particles.

For the coal samples in Table 6.2, the greater dependence of the ϵ' values estimated by the Böttcher and Bruggeman-Hanai equations on volume fraction of the Dahm sample, compared to the Illinois #6 sample, could be due to differences in particle size distribution for the two different coals. Particle sizes of the Illinois #6 coal sample are somewhat more uniformly distributed across the entire size range, even though the largest portion of the particles is very fine.

No apparent differences in particle size distribution are evident in Table 6.7 that might contribute to the difference noted between goethite and the silicates in Table 6.3. Also, the particle size distribution of the ilmenite sample does not appear different enough from those of the goethite or silicate samples to account for the notable difference in the predicted ϵ' values of the Böttcher equation, relative to the other mixture equations for ilmenite and the minerals of Table 6.3.

The mixture equations (2) through (5) are based on the assumption of spherically shaped particles. A number of generalizations of these equations have been developed for particles of ellipsoidal and other shapes [10], [11], [15], [31], [50]. Equations (1) and (6) have a less rigorous theoretical basis and have generally been considered applicable for particles of arbitrary shape. The materials represented in Tables 6.1 to 6.4 certainly did not have spherical particles. Except for the whole-grain wheat, neither can they be characterized by any other uniform shape. When viewed under a microscope, most of them appeared to be broken chunks of irregular shape with a wide range of sizes as evidenced by the data of Tables 6.5 to 6.7. Only the phlogopite mica and the chlorite particles had a distinct flake-like appearance in the larger sizes, and many of the fine particles did not readily exhibit the thin dimension. The goethite sample had some large needle-shaped and small splinter-like particles mixed with the other irregularly shaped fine particles.

At the two higher frequencies, those above 10 GHz, scattering effects may need to be taken into account, particularly with the larger particles [51–52]. Maxwell-Wagner losses [11], [15], [53] may also need to be taken into account with some of these particulate materials, although these effects would normally be expected to take on significance at lower frequencies.

c. Comparison of Predicted with Known Permittivities

The comparisons on the various materials represented in Tables 6.1 through 6.4 are frustrated by the lack of known permittivities for the solid materials. Therefore, it is difficult to select the most reliable equation or method of estimating the properties of the solid materials. For this reason some additional measurements and analyses were conducted on two plastics for which suitable samples could be prepared for permittivity measurements on both the solid and the particulate forms.

Samples of Rexolite 1422*, a low-loss thermoset cross-linked styrene copolymer used for high-frequency insulating components, and of Kynar, polyvinylidene fluoride (PVDF), a thermoplastic with high chemical resistance and relatively high dielectric loss, were machined for the 21-mm coaxial line and the WR-90 and WR-42 rectangular waveguide sample holders used for the measurements on the other particulate materials. Fine particles of these materials were obtained by grinding shavings from the lathe work on the solid samples in a Thomas-Wiley intermediate laboratory mill to pass through a No. 40 mesh screen (0.38 mm openings). Permittivity measurements were taken at 2.45, 11.5, and 22.0 GHz by methods already described, and the data were processed in the same way that has been explained for the other materials. Results of these measurements are summarized in Tables 6.8 and 6.9.

For Rexolite 1422 at 2.45 GHz, the square-root extrapolation and the Refractive Index mixture equation slightly underestimated the dielectric constant, whereas the cube-root extrapolation and the Landau and Lifshitz, Looyenga equation overestimated it by a similar error, about 1%. The cube-root extrapolation and Landau and Lifshitz, Looyenga equation estimates for ϵ' were very close at 11.5 GHz, where

* Mention of company or trade names is for purpose of description only and does not imply endorsement by the U. S. Department of Agriculture.

the square-root and Refractive Index equation gave an estimate about 1.5% low. At 22 GHz all of these methods gave slightly low values of ϵ'. Loss factor estimates by the extrapolation technique were relatively close.

The Böttcher and Landau and Lifshitz, Looyenga equations agreed very closely in their estimates of the permittivity of the solid material, whereas the Bruggeman-Hanai, Rayleigh, and Lichtenecker equations gave increasingly larger values in that order. Relatively little dependence on the volume fraction was exhibited by the mixture equations in their estimates of the solid material dielectric constant. At 11.5 and 22 GHz, a tendency is noted for loss factors to increase with higher volume fractions.

For Kynar (Table 6.9), all methods of solid material permittivity estimation, except the Refractive Index equation at low volume fractions, gave values of ϵ' larger than the measured values for the solid material specimens. Since the cube-root extrapolation and Landau and Lifshitz, Looyenga equation customarily give higher estimates than the square-root extrapolation and the Refractive Index equation, the latter provided the closest estimate, which was about 4% too large. The Bruggeman-Hanai, Rayleigh, and Lichtenecker equations gave increasingly larger estimates of solid material permittivity in the order listed. Scattering effects could account for the slightly higher overestimation of the solid material permittivity by the measurements on particulate samples at 22 GHz. If the effective permittivity measured on the particulate samples included a scattering component, the solid permittivity would be estimated too high.

The extrapolated value for ϵ'' at 22 GHz was very close to the measured value, but the extrapolated values at 2.45 and 11.5 GHz were slightly too high. The Refractive Index equation gave better ϵ'' estimates for the solid material at these two frequencies.

Differences in the performance of the methods for estimating permittivities of the solid materials from measurements on the particulate forms prompted a microscopic examination of the particles of Rexolite 1422 and Kynar and a determination of particle-size distribution. Particle size results are given in Table 6.10. The microscopic examination revealed marked differences in the shapes of the particles for the two materials. Whereas the Rexolite 1422 particles appeared to have been chopped and broken into irregularly shaped particles, the Kynar particles appeared to consist of more thin, flake-like, curled, extruded

and torn particles, as if heat generated in the grinding process had softened the solid material. The marked contrast in the shapes of the particles of the two different materials might account for differences in the behavior of the particulate materials with respect to the use of the mixture equations and the extrapolation method for estimating the permittivity of the solid material.

6.7 Conclusions

A method is presented for extrapolating linear functions of the real and imaginary parts of the complex relative permittivity of air-particle mixtures measured at several different mixture densities to obtain estimates of the permittivity of the solid material. Linearity of the square root of the real part (dielectric constant) with mixture density is consistent with the Refractive Index mixture equation, and linearity of the cube-root of the dielectric constant with mixture density is consistent with the Landau and Lifshitz, Looyenga mixture equation. Linearity with mixture density of the square root of the imaginary part of the complex relative permittivity (loss factor), after a small constant is added, is consistent with quadratic dependence of the loss factor on density and is therefore consistent with the linearity, with density, of the square root of the complex permittivity. This implies consistency between the linearity with density of this function of the loss factor and the Refractive Index mixture equation applied to the complex permittivity.

Application of the mixture equations to some particulate materials reveals a dependence of the estimated permittivity on the volume fraction at which data are taken on the particulate material. The extrapolation procedure averages this variation. If the mixture equations are applied to estimate the solid material permittivity, measurements should be taken at more than one density of the particulate material.

On the basis of the limited experimental evidence presented for materials of known solid material permittivities, the Refractive Index and Landau and Lifshitz, Looyenga mixture equations appear to be the most reliable equations for estimating solid material permittivities from measurements on these particulate materials. The Böttcher equation often gave values very close to those of the Landau and Lifshitz, Looyenga equation. The Bruggeman-Hanai, Rayleigh, and Lichtenecker mixture equations gave estimated permittivities of increasing magnitude in the order listed for the particulate Rexolite 1422 and Ky-

nar plastic materials. For whole-kernel wheat, ground wheat, ground rice, pulverized coal and the pulverized silicate minerals, chlorite and feldspar, the order of the Rayleigh and Lichtenecker equations was reversed. For mica and the metal oxide minerals, goethite and ilmenite, the Lichtenecker equation gave better values than the Bruggeman-Hanai equation.

The best selection from the various mixture equations depends on the particular material of interest. Results appear to be dependent on the particle size and the particle size distribution. Further study is required to provide a better understanding of the influence of various factors. The data are presented here in tabular form, along with available information on particle size distributions, in hope that they may be useful* to those interested in clarifying the use of mixture equations for determining solid material permittivity from measurements on particulate materials.

Acknowledgments

The author is grateful to Tian-su You for assistance with the new measurements on Rexolite 1422 and Kynar samples and to Bruce Cantrell, Thomas McCartney, and Rolland Blake of the U.S. Bureau of Mines for furnishing the Leeds and Northrup Microtrack 7981 particle size analysis on these samples and the mineral samples. He is also indebted to Andrzej Kraszewski, Mike Kent, Alain Priou, and Wayne Tinga for review of the manuscript and helpful suggestions.

* Tabulations of unrounded measurement data on the permittivity and volume fractions for samples included in this article can be furnished upon request.

References

[1] Böttcher, C. J. F., "The dielectric constant of crystalline powders," *Rec. Trav. Chim.*, **64**, 47–51, 1945.

[2] Dube, D. C., and R. Parshad, "Study of Böttcher's formula for dielectric correlation between powder and bulk," *J. Phys. D: App. Phys.*, **3**, 677–684, 1970.

[3] Dube. D. C., "Study of Landau-Lifshitz-Looyenga's formula for dielectric correlation between powder and bulk," *J. Phys. D: Appl. Phys.*, **3**, 1648–1652, 1970.

[4] Yadav, A. S., and R. Parshad, "On the utilization of Böttcher's formula for correct correlation of dielectric constant of powder and bulk," *J. Phys. D: Appl. Phys.*, **4**, 822–824, 1971.

[5] Dube, D. C., R. S. Yadava, and R. Parshad, "A formula for correlating dielectric constant of powder and bulk," *Indian J. Pure & Appl. Phys.*, Vol. 9, 719–721, 1971.

[6] Nelson, S. O., "Method for determining dielectric properties of solids from measurements on pulverized materials," *1987 IEEE MTT-S Internat'l. Microwave Symp. Digest*, **1**, 461–463, 1987.

[7] Nelson, S. O., "Estimating the permittivity of solids from measurements on granular or pulverized materials," *Materials Res. Soc. Symp. Proc.*, Vol. 124, 149–154, 1988.

[8] De Loor, G. P., "Dielectric properties of heterogeneous mixtures," Thesis, Univ. Leiden, 1956.

[9] Reynolds, J. A., and J. M. Hough, "Formula for dielectric constant of mixtures", *Proc. Phys. Soc.*, Vol. 70, 769–775, 1957.

[10] van Beek, L. K. H., "Dielectric behavior of heterogeneous systems," In J. B. Birks, Ed., *Progress in Dielectric*, Vol. 7, 69–114, Heywood Books, London, 1967.

[11] Dukhin, S. S., "Dielectric properties of disperse systems", In E. Matijevic, Ed., *Surface and Colloid Science*, **3**, 83–164, Wiley-Interscience, New York, 1971.

[12] Tinga, W. R., W. A. G. Voss, and D. F. Blossey, "Generalized approach to multiphase dielectric mixture theory," J. Appl. Phys., 44, 3897–3902, 1973.

[13] Tareev, B., *Physics of Dielectric Materials,* A. Troitsky, Transl., 1973 Russian Ed., Mir Publ., Moscow, 1975.

[14] Kraszewski, A. "Prediction of the dielectric properties of two-phase mixtures," *J. Microwave Power,* Vol. 12, 215–222, 1977.

[15] Böttcher, C. J. F., and P. Bordewijk, *Theory of Electric Polarization, Vol. II,* Elsevier Sci. Publ. Co., Amsterdam, 1978.

[16] Grosse, C., and J. L. Greffe, "Permittivities statique des emulsions," *J. Chimie Physique,* **76**, 305–327, 1979.

[17] Beer, A. *Einleitung in die Höhere Optik,* 35, F. Vieweg und Sohn, Braunschweig, 1853.

[18] Gladstone, J. H., and T. P. Dale, "Researches on the refraction, dispersion, and sensitiveness of liquids," *Phil. Trans.,* **153**, 317–343, 1863.

[19] Lichtenecker, K., "Die Dieletrizitätskonstante natürlicher und küstlicher Mischkörper," *Phys. Zeitschr.,* **27**, 115–158, 1926.

[20] Birchak, J. R., C. Gardner, J. E. Hipp, and J. M. Victor, "High dielectric constant microwave probes for sensing soil moisture content," *Proc. IEEE,* **62**, 93–98, 1974.

[21] Kraszewski, A., S. Kulinski, and M. Matuszewski, "Dielectric properties and a model of biphase water suspension at 9.4 GHz," *J. Appl. Phys.,* **47**, 1275–1277, 1976.

[22] Philip, J. C., "Das dielektrische Verhalten flössiger Mischungen, besonders verdünter Lösungen," *Z. Physik. Chemie,* **24**, 18–38, 1897.

[23] Lowry, H. H., "The significance of the dielectric constant of a mixture," *J. Franklin Inst.,* **203**, 413–439, 1927.

[24] Calderwood, J. H., and B. K. P. Scaife, "On the estimation of the relative permittivity of a mixture," *IEE Conf. Publ. No. 177,* 136–139, 1979.

[25] Shutko, A. M., and E. M. Reutov, "Mixture formulas applied in estimation of dielectric and radiative characteristics of soils and grounds at microwave frequencies," *IEEE Trans. Geosci. Remote Sens.,* **GE-20**, 29–32, 1982.

[26] Shen, L. C., W. C. Savre, J. M. Price, and K. Athavale, "Dielectric properties of reservoir rocks at ultra-high frequencies," *Geophys.,*

50, 692–704, 1985.

[27] Feng, S. and P. N. Sen, "Geometrical model of conductive and dielectric properties of partially saturated rocks," *J. Appl. Phys.*, **58**, 3236–3243, 1985.

[28] Landau, L. D., and E. M. Lifshitz, *Electrodynamics of Continuous Media*, Pergamon Press, Oxford, 1960.

[29] Looyenga, H., "Dielectric constants of heterogeneous mixtures," *Physica*, **31**, 401–406, 1965.

[30] Nelson, S. O., "Observations on the density dependence of the dielectric properties of particulate materials," *J. Microwave Power*, **18**, 143–152, 1983.

[31] Banhegyi, G., "Numerical analysis of complex dielectric mixture formulae," *Coll. Polymer Sci.*, **266**, 11–28, 1988.

[32] Bruggeman, D. A. G., "Berechnung verschiedener physikalischer Konstanten von heterogenen Substanzen. I. Dielektrizitätskonstanten und Leitfähigkeiten der Mischkörper aus isotropen Substanzen," *Ann. der Phys.*, **24**, 636–664, 1935.

[33] Hanai, T., "Theory of the dielectric dispersion due to the interfacial polarization and its application to emulsions," *Koll. Zeitschr.*, **171**, 23–31, 1960.

[34] Rayleigh, Lord, "On the influence of obstacles arranged in rectangular order upon the properties of a medium," *Phil. Mag.*, **34**, 481–502, 1892.

[35] Lichtenecker, K., and K. Rother, "Die Herleitung des logarithmischen Mischungsgesetzes aus allgemeinen Prinzipien der stationären Strömung, *Phys. Zeitschr.*, **32**, 255–260, 1931.

[36] Klein, A., "Microwave determination of moisture in coal—a comparison of attentuation and phase measurement," *J. Microwave Power*, **16**, 289–304, 1981.

[37] Kent, M., "Complex permittivity of fish meal: a general discussion of temperature, density, and moisture dependence," J. Microwave Power, **12**, 341–345, 1977.

[38] Nelson, S. O., S. R. Beck-Montgomery, G. E. Fanslow, and D. D. Bluhm, "Frequency dependence of the dielectric properties of coal – Part II," *J. Microwave Power*, **16**, 319–326, 1981.

[39] Roberts, S., and A. von Hippel, "A new method for measuring dielectric constant and loss in the range of centimeter waves," *J. Appl. Phys.*, **17**, 610–616, 1946.

[40] Nelson, S. O., C. W. Schlaphoff, and L. E. Stetson, "Computer program for calculating dielectric properties of low- or high-loss materials from short-circuited waveguide measurements," *U. S. Dept. Agric., Agric. Res. Ser., Rept. No. ARS-NC-4*, 1972.

[41] Nelson, S. O., L. E. Stetson, and C. W. Schlaphoff, "A general computer program for precise calculation of dielectric properties from short-circuited-waveguide measurements," *IEEE Trans. Instr. Meas.*, **IM-23**, 455–460, 1974.

[42] Nelson, S. O., "Microwave dielectric properties of grain and seed," *Trans. ASAE*, **16**, 902–905, 1973.

[43] Nelson, S. O., "A system for measuring dielectric properties at frequencies from 8.2 to 12.4 GHz," *Trans. ASAE*, **15**, 1094–1098, 1972.

[44] Nelson, S. O., and T. S. You, "Dielectric properties of corn and wheat kernels and soybeans at microwave frequencies," *Trans. ASAE*, **32**, 242–249, 1989.

[45] Nelson, S. O., "Dielectric properties of some fresh fruits and vegetables at frequencies of 2.45 to 22 GHz," *Trans. ASAE*, **26**, 613–616, 1983.

[46] You, T. S., and S. O. Nelson, "Microwave dielectric properties of rice kernels," *J. Microwave Power*, **23**, 150–159, 1988.

[47] Nelson, S. O., D. P. Lindroth, and R. L. Blake, "Dielectric properties of selected minerals at 1 to 22 GHz," *Geophysics*, **54**, 1344–1349, 1989.

[48] Nelson, S. O., "Models for the dielectric constants of cereal grains and soybeans," *J. Microwave Power*, **22**, 35–39, 1987.

[49] Nelson, S. O., G. E. Fanslow, and D. D. Bluhm, "Frequency dependence of the dielectric properties of coal," *J. Microwave Power*, **15**, 277–282, 1980.

[50] Sen, P. N., C. Scala, and M. H. Cohen, "A self-similar model for sedimentary rocks with application to the dielectric constant of fused glass beads," *Geophys.*, **46**, 781–795, 1981.

[51] Kong, J. A., *Electromagnetic Wave Theory,* Wiley-Interscience, New York, 1986.

[52] Sihvola, A. H., and J. A. Kong, "Effective permittivity of dielectric mixtures," *IEEE Trans. Geosci. Remote Sensing,* **26**, 420–429, 1988.

[53] Daniel, V. V., *Dielectric Relaxation,* Academic Press, London, 1967.